Acta Cryst E CRYSTALLOGRAPHIC COMMUNICATIONS
ISSN 2056-9890

6-Methyl-2-oxo-*N*-(quinolin-6-yl)-2*H*-chromene-3-carboxamide: crystal structure and Hirshfeld surface analysis

Lígia R. Gomes,[a,b] John Nicolson Low,[c]* André Fonseca,[d] Maria João Matos[d] and Fernanda Borges[d]

[a]FP–ENAS–Faculdade de Ciências de Saúde, Escola Superior de Saúde da UFP, Universidade Fernando Pessoa, Rua Carlos da Maia, 296, P-4200-150 Porto, Portugal, [b]REQUIMTE, Departamento de Química e Bioquímica, Faculdade de Ciências da Universidade do Porto, Rua do Campo Alegre, 687, P-4169-007 Porto, Portugal, [c]Department of Chemistry, University of Aberdeen, Meston Walk, Old Aberdeen AB24 3UE, Scotland, and [d]CIQUP/Departamento de Química e Bioquímica, Faculdade de Ciências, Universidade do Porto, 4169-007 Porto, Portugal. *Correspondence e-mail: jnlow111@gmail.com

Received 1 July 2016
Accepted 7 July 2016

Edited by W. T. A. Harrison, University of Aberdeen, Scotland

Keywords: crystal structure; coumarin; carboxamide; Hirshfeld surface analysis.

CCDC reference: 1491340

Supporting information: this article has supporting information at journals.iucr.org/e

The title coumarin derivative, $C_{20}H_{14}N_2O_3$, displays intramolecular N—H···O and weak C—H···O hydrogen bonds, which probably contribute to the approximate planarity of the molecule [dihedral angle between the coumarin and quinoline ring systems = 6.08 (6)°]. The supramolecular structures feature C—H···O hydrogen bonds and π–π interactions, as confirmed by Hirshfeld surface analyses.

1. Chemical context

Coumarin and its derivatives are widely recognized by their unique biological properties (Matos *et al.*, 2014; Vazquez-Rodriguez *et al.*, 2013; Chimenti *et al.*, 2010). Our work in this area has shown that coumarin is a valid scaffold for the development of new drugs for aging related diseases, specifically within the class of monoamino oxidase B inhibitors (Matos *et al.*, 2009). On the other hand, quinoline is a nitrogen heterocycle also often used in drug-discovery programs due to its remarkable biological properties, some of them related to neurodegenerative diseases (Sridharan *et al.*, 2011), for instance, as γ-secretase and acetylcholinesterase inhibitors (Camps *et al.*, 2009). As part of our ongoing studies in this area (Gomes *et al.*, 2016), we describe the synthesis and crystal structure of the title coumarin–quinoline hybrid, 6-methyl-2-oxo-*N*-(quinolin-6-yl)-2*H*-chromene-3-carboxamide, (1) (see Scheme).

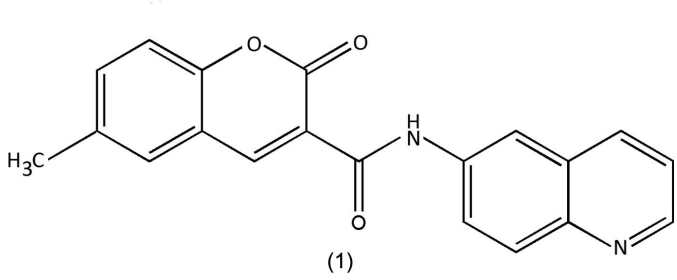

(1)

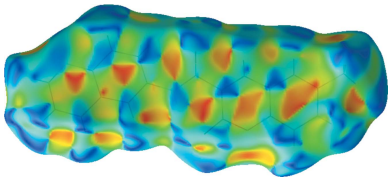

2. Structural commentary

Fig. 1 shows an ellipsoid plot of the molecular structure of (1). An inspection of the bond lengths shows that there is a slight

Table 1
Hydrogen-bond geometry (Å, °).

D—H···A	D—H	H···A	D···A	D—H···A
C314—H314···O31^{i}	0.95	2.50	3.278 (2)	139
C8—H8···N311^{ii}	0.95	2.68	3.394 (3)	133
C317—H317···O31	0.95	2.29	2.903 (2)	122
N32—H32···O2	0.907 (18)	1.879 (18)	2.686 (2)	147.3 (15)

Symmetry codes: (i) $x+1, y, z$; (ii) $x-\frac{1}{2}, -y+\frac{1}{2}, z-\frac{1}{2}$; (iii) $x-1, y, z$.

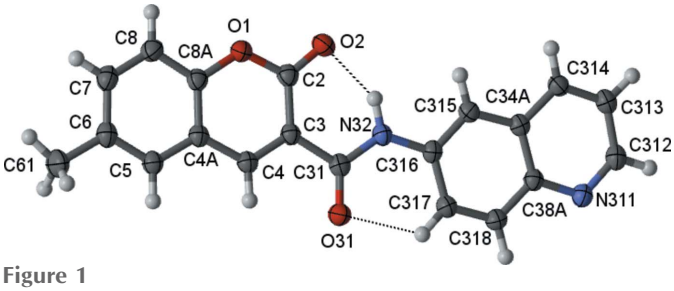

Figure 1
A view of the asymmetric unit of (1), showing the atom-numbering scheme. Displacement ellipsoids are drawn at the 70% probability level.

asymmetry of the electronic distribution around the coumarin ring: the C3—C4 [1.3609 (15) Å] and C3—C2 [1.4600 (18) Å)] bond lengths are shorter and longer, respectively, than those expected for a C_{ar}—C_{ar} bond, suggesting that the electronic density is rather located near the C3—C4 bond at the pyrone ring, as occurs in other coumarin-3-carboxamide derivatives (Gomes *et al.*, 2016). Also, the C3—C31 bond length [1.5075 (18) Å] is similar to the mean value displayed by other coumarin-3-carboxamide derivatives previously characterized (Gomes *et al.*, 2016) and is of the same order as a Csp^3—Csp^3 bond.

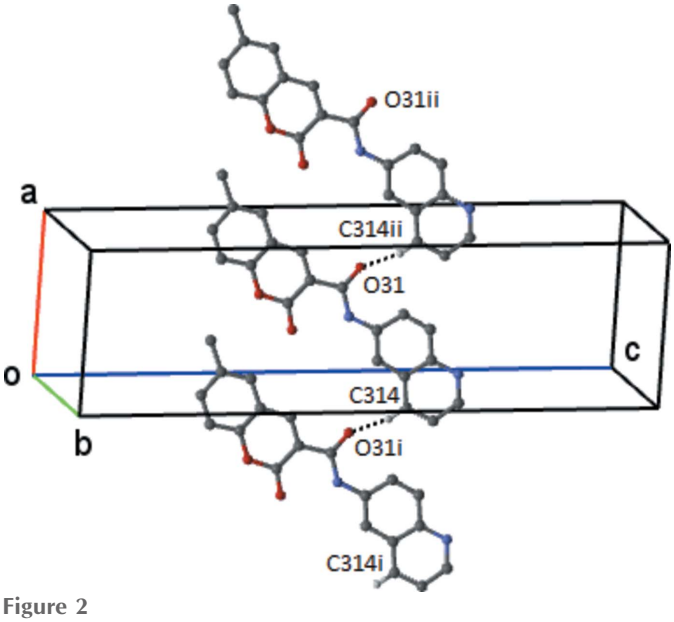

Figure 2
The simple *C*4 chain in compound (1) formed by the weak C314—H314···O3^{i} hydrogen bond. This chain extends by unit translation along the *a* axis. H atoms not involved in the hydrogen bonding have been omitted. [Symmetry codes: (i) $x-1, y, z$; (ii) $x+1, y, z$.]

Table 2
Selected dihedral angles (°).

Compound	θ_1 (°)	θ_2 (°)	θ_3 (°)
(1)	6.08 (6)	5.0 (12)	1.73 (11)

Notes: θ_1 is the dihedral angle between the mean planes of the coumarin and quinoline rings; θ_2 is the dihedral angle between the mean plane of the coumarin ring and the plane defined by atoms O31/C31/N32; θ_3 is the dihedral angle between the mean plane of the quinoline ring and the plane defined by atoms O31/C31/N32.

The C—N rotamer of the amide group governs the conformation of the molecule: the *−anti* orientation where the N atom is *−cis* positioned with respect to the oxo O atom of the coumarin system allows the establishment of an intramolecular N32—H32···O2 hydrogen bond between the amino group of the carboxamide and the oxo group of the coumarin system, and of a weak intramolecular C317—H317···O31 hydrogen bond that connects the quinoline ring with the O atom of the carboxamide group (Table 1). Both these interactions form *S*(6) rings and connect the spacer carboxamide group with the heteroaromatic rings, probably constraining the rotation/bending of those rings with respect to the plane formed by the amide atoms. In fact, the molecule is roughly planar, as may be evaluated by the set of values for the dihedral angles which are less than 7° (Table 2).

3. Supramolecular features

In the crystal of (1), molecules are linked by a weak C314—H314···O31^{i} hydrogen bond to form a *C*(8) chain, which runs parallel to the *a* axis (Fig. 2 and Table 1). There are several π–π contacts that will be described below.

4. Hirshfeld surface analyses

The Hirshfeld surfaces and two-dimensional fingerprint (FP) plots (Rohl *et al.*, 2008) were generated using *Crystal Explorer* (Wolff *et al.*, 2012). Compound (1) has three O atoms and an N atom that can potentially act as acceptors for hydrogen bonds, but one of the lone pairs of the oxo O atoms of the coumarin nucleus and of the amide moiety are involved in the establishment of intramolecular hydrogen bonds, as discussed above. As such, they contribute to the electronic density of the pro-molecule in the calculation of the Hirshfeld surface, leaving only the remaining pairs available for participation in the supramolecular structure formation. The surface mapped over d_{norm} displays several red spots that correspond to areas of close contacts between the surface and the neighbouring environment, and the FP plot is presented in Fig. 3.

The contributions from various contacts, listed in Table 3, were selected by partial analysis of the FP plot. Taking out the H···H contacts on the surface that are inherent to organic molecules, the most significant contacts can be divided in three groups: (i) H···O/O···H together with H···N/N···H that correspond to weak C—H···O/N intermolecular interactions (24.5%); (ii) C···C and N···C/C···N contacts that are related

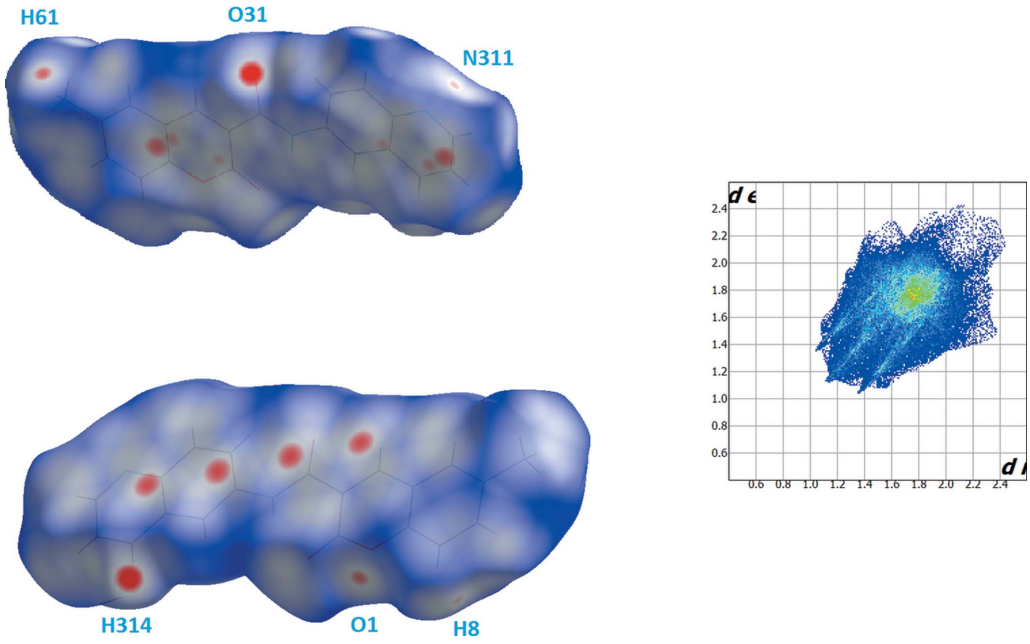

Figure 3
Views of the Hirshfeld surface mapped over d_{norm} (left) and fingerprint plot (right, FP) for (1). The highlighted red spots on the top face of the surfaces indicate contact points with the atoms participating in the intermolecular C—H···O interactions, whereas those on the middle of the surface corresponds to C···C contacts consequent of the π–π stacking. The C···C contacts contribute to the higher frequency of the pixels at d_e/d_i at 1.8° on the FP plot (yellow spot). The FP plot displays two light-blue spikes (external ends corresponding to C··· H contacts).

with π–π stacking (17.9%): (iii) H···C/C···H contacts (14.3%).

The H···N/O contacts appear as three highlighted red spots on the top and bottom edges of the surface which form pairs of spots of comlementary size, indicating the contact points of the

Table 3
Percentages of atom–atom contacts for (1) (%).

Contact	H···H	H···O/ O···H	H···N/ N···H	C···C	N···C/ C···N	H···C/ C···H
(%)	40.6	21.2	3.3	13.2	4.7	14.3

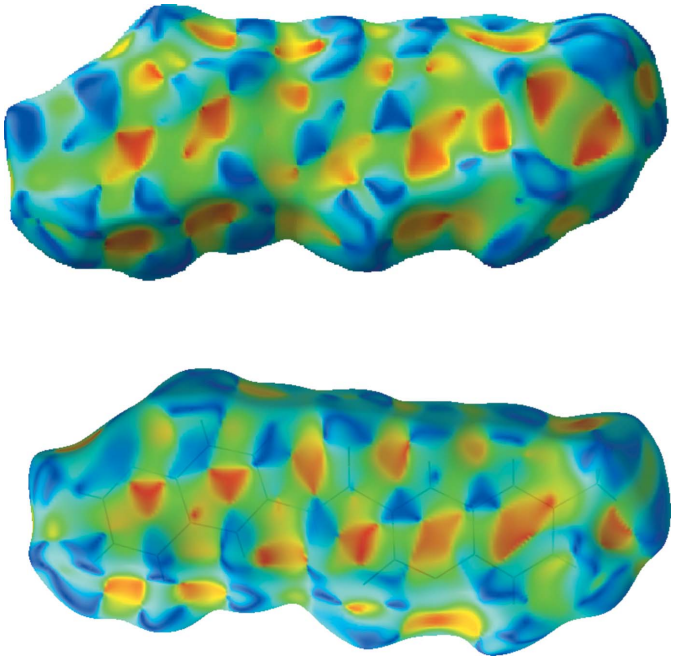

Figure 4
Shape index plots showing the interactions arising from π–π stacking. The upper corresponds to the stacking across ($\frac{1}{2}$, 1, $\frac{1}{2}$), while the lower corresponds to the stacking across ($\frac{1}{2}$, $\frac{1}{2}$, $\frac{1}{2}$).

labelled atoms participating in the C–H···N/O interactions (Fig. 3). The strongest spots correspond to oxo atom O31 of the carboxamide acceptor and donor atom H314, which forms the C314—H314···O31^{i} hydrogen bond (Table 1), and the other spots correspond to very weak hydrogen-bond contacts, one involving pyrone atom O1 and a H atom of the methyl group (C61—H61*B*···O1^{ii}; Table 1), and the other appearing perpendicular to the quinoline N atom indicating a very weak C8—H8···N311^{ii} contact (Table 1). In spite of the weakness of these contacts, their relative strength is reflected in the FP plots where the pair of sharp spikes pointing to south-west is highlighted in light blue.

In this structure, C/N···C contacts prevail over the C—H···C ones. In fact, the packing in (1) is built up by several π–π interactions (Table 4). The red spots in the frontal zone of the surface correspond to these close contacts. Furthermore, the FP plot also reveals an intense cluster at d_e/d_i at 1.8 Å characteristic of C···C contacts. Also, when the surface is mapped with shape index, several complementary triangular red hollows and blue bumps appear that are characteristic of the six-ring stacking (Fig. 4). The molecules stack in a column in a head-to-tail fashion along the *b* axis (Fig. 5). The molecules in these stacks lie across centres of symmetry at ($\frac{1}{2}$, 1, $\frac{1}{2}$),

Table 4
Selected π–π contacts.

Compound	*CgI*	*CgJ*(aru)	*Cg*–*Cg* (Å)	*CgI*_Perp (Å)	*CgJ*_Perp (Å)	Slippage (Å)
1	*Cg*1	*Cg*2($-x+1, -y, -z-1$)	3.548 (2)	3.1477 (4)	3.3051 (4)	1.290
1	*Cg*1	*Cg*2($-x+1, -y+1, -z-1$)	3.911 (3)	−3.3848 (4)	−3.3352 (4)	2.043
1	*Cg*1	*Cg*4($-x+1, -y+1, -z-1$)	3.525 (2)	−3.3851 (4)	−3.2952 (4)	1.252
1	*Cg*2	*Cg*1($-x+1, -y, -z-1$)	3.548 (2)	3.3050 (4)	3.1476 (4)	1.637
1	*Cg*2	*Cg*1($-x+1, -y+1, -z-1$)	3.911 (3)	−3.3352 (4)	−3.3849 (4)	1.960
1	*Cg*2	*Cg*3($-x+1, -y+1, -z-1$)	3.797 (3)	−3.3389 (4)	−3.5276 (5)	1.406
1	*Cg*3	*Cg*2($-x+1, -y+1, -z-1$)	3.798 (3)	−3.5277 (5)	−3.3388 (4)	1.809
1	*Cg*4	*Cg*1($-x+1, -y+1, -z-1$)	3.525 (2)	−3.2951 (4)	−3.3852 (4)	0.983

Notes: *CgI*(*J*) = Plane number *I*(*J*); *Cg*–*Cg* = distance between ring centroids; *CgI*_Perp = perpendicular distance of *CgI* on ring *J*; *CgJ*_Perp = perpendicular distance of *CgJ* on ring *I*; Slippage = distance between *CgI* and perpendicular projection of *CgJ* on ring *I*.Plane 1 is the plane of the coumarin pyran ring with *Cg*1 as centroid; Plane 2 is the plane of the quinoline pyridine ring with *Cg*2 as centroid; Plane 3 is the plane of the coumarin phenyl ring with *Cg*3 as centroid; Plane 4 is the plane of the quinoline phenyl ring with *Cg*4 as centroid.Some planes are repeated since they are inclined to each other and as a result give slightly different slippages

Table 5
Experimental details.

Crystal data	
Chemical formula	$C_{20}H_{14}N_2O_3$
M_r	330.33
Crystal system, space group	Monoclinic, $P2_1/n$
Temperature (K)	100
a, b, c (Å)	7.799 (3), 7.014 (3), 27.640 (18)
β (°)	90.18 (6)
V (Å^3)	1512.0 (13)
Z	4
Radiation type	Synchrotron, λ = 0.68891 Å
μ (mm^{-1})	0.09
Crystal size (mm)	0.18 × 0.01 × 0.004
Data collection	
Diffractometer	Three-circle diffractometer
Absorption correction	Empirical (using intensity measurements) (aimless *CCP4*; Evans, 2006)
No. of measured, independent and observed [$I > 2\sigma(I)$] reflections	18408, 4587, 3717
R_{int}	0.060
(sin $\theta/\lambda)_{max}$ (Å^{-1})	0.714
Refinement	
$R[F^2 > 2\sigma(F^2)]$, $wR(F^2)$, S	0.051, 0.156, 1.13
No. of reflections	4587
No. of parameters	231
H-atom treatment	H atoms treated by a mixture of independent and constrained refinement
$\Delta\rho_{max}$, $\Delta\rho_{min}$ (e Å^{-3})	0.54, −0.25

Computer programs: GDA http://www.opengda.org/OpenGDA.html, XIA2 0.4.0.370-g47f3bc3 (Winter, 2010), *SHELXT* (Sheldrick, 2015*a*), ShelXle (Hübschle *et al.*, 2011), *SHELXL2014* (Sheldrick, 2015*b*), *Mercury* (Macrae *et al.*, 2006) and *PLATON* (Spek, 2009).

a centrosymetrically related contact between the pyran and pyridine rings, and across the centre at $(\frac{1}{2}, \frac{1}{2}, \frac{1}{2})$, which involves three short centrosymmetrically related contacts: (i) between the pyran and pyridine rings, (ii) between the pyran ring and the quinoline phenyl ring and (iii) between the coumarin phenyl ring and the pyridine ring.

5. Database survey

As reported by Gomes *et al.* (2016), a search made in the Cambridge Structural Database (CSD, Version 35.7; Groom *et al.*, 2016) revealed the existence of 35 deposited compounds (42 molecules) containing the coumarin carboxamide unit, all of which contained the same intramolecular hydrogen bonds. The present compound also contains these bonds, as described above.

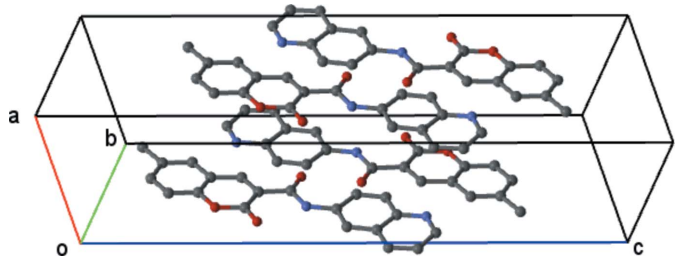

Figure 5
View of the π–π stacking along the *b* axis.

6. Synthesis and crystallization

6-Methylcoumarin-3-carboxylic acid (Murata *et al.*., 2005) (1 mmol) was dissolved in dichloromethane and 3-[3-(dimethylamino)propyl]-1-ethylcarbodiimide (1.10 mmol) and 4-dimethylaminopyridine (1.10 mmol) were added. The mixture was kept under a flux of argon at 273 K for 5 min. 6-Aminoquinoline (1 mmol) was then added in small portions. The reaction mixture was stirred for 4 h at room temperature. The obtained precipitate was filtered off and recrystallized from methanol to give colourless needles of (1). Overall yield: 53%; m.p. 545–546 K.

7. Refinement

H atoms were treated as riding atoms, with aromatic C—H = 0.95 Å, with U_{iso}(H) = 1.2U_{eq}(C), and methyl C—H = 0.98 Å, with U_{iso}(H) = 1.5U_{eq}(C). The amino H atoms were freely refined. Crystal data, data collection and structure refinement details are summarized in Table 5.

Acknowledgements

The authors thank the staff at the National Crystallographic Service, University of Southampton, for the data collection, help and advice (Coles & Gale, 2012), and the Foundation for Science and Technology (FCT) and FEDER/COMPETE2020 (UID/QU*i*00081/2015 and POCI-01–0145-FEDER-006980). AF (SFRH/BD/80831/2011) and MJM (SFRH/BPD/95345/2013) were supported by grants from FCT, POPH and QREN.

References

Camps, P., Formosa, X., Galdeano, C., Muñoz-Torrero, D., Ramírez, L., Gómez, E., Isambert, N., Lavilla, R., Badia, A., Clos, M. V., Bartolini, M., Mancini, F., Andrisano, V., Arce, M. P., Rodríguez-Franco, M. I., Huertas, O., Dafni, T. & Luque, F. J. (2009). *J. Med. Chem.* **52**, 5365–5379.

Chimenti, F., Bizzarri, B., Bolasco, A., Secci, D., Chimenti, P., Granese, A., Carradori, S., Rivanera, D., Zicari, A., Scaltrito, M. M. & Sisto, F. (2010). *Bioorg. Med. Chem. Lett.* **20**, 4922–4926.

Coles, S. J. & Gale, P. A. (2012). *Chem. Sci.* **3**, 683–689.

Evans, P. (2006). *Acta Cryst.* D**62**, 72–82.

Gomes, L. R., Low, J. N., Fonseca, A., Matos, M. J. & Borges, F. (2016). *Acta Cryst.* E**72**, 926–932.

Groom, C. R., Bruno, I. J., Lightfoot, M. P. & Ward, S. C. (2016). *Acta Cryst.* B**72**, 171–179.

Hübschle, C. B., Sheldrick, G. M. & Dittrich, B. (2011). *J. Appl. Cryst.* **44**, 1281–1284.

Macrae, C. F., Edgington, P. R., McCabe, P., Pidcock, E., Shields, G. P., Taylor, R., Towler, M. & van de Streek, J. (2006). *J. Appl. Cryst.* **39**, 453–457.

Matos, M. J., Janeiro, P., Gonz\'alez Franco, R. M., Vilar, S., Tatonetti, N. P., Santana, L., Uriarte, E., Borges, F., Fontenla, J. A. & Viña, D. (2014). *Future Med. Chem.* **6**, 371–383.

Matos, M. J., Viña, D., Quezada, E., Picciau, C., Delogu, G., Orallo, F., Santana, L. & Uriarte, E. (2009). *Bioorg. Med. Chem. Lett.* **19**, 3268–3270.

Murata, C., Masuda, T., Kamochi, Y., Todoroki, K., Yoshida, H., Nohta, H., Yamaguchi, M. & Takadate, A. (2005). *Chem. Pharm. Bull. (Tokyo)*, **53**, 750–758.

Rohl, A. L., Moret, M., Kaminsky, W., Claborn, K., McKinnon, J. J. & Kahr, B. (2008). *Cryst. Growth Des.* **8**, 451–4525.

Sheldrick, G. M. (2015*a*). *Acta Cryst.* A**71**, 3–8.

Sheldrick, G. M. (2015*b*). *Acta Cryst.* C**71**, 3–8.

Spek, A. L. (2009). *Acta Cryst.* D**65**, 148–155.

Sridharan, V., Suryavanshi, P. & Menéndez, J. C. (2011). *Chem. Rev.* **111**, 7157–7259.

Vazquez-Rodriguez, S., Matos, M. J., Santana, L., Uriarte, E., Borges, F., Kachler, S. & Klotz, K. N. (2013). *J. Pharm. Pharmacol.* **65**, 607–703.

Winter, G. (2010). *J. Appl. Cryst.* **43**, 186–190.

Wolff, S. K., Grimwood, D. J., McKinnon, J. J., Turner, M. J., Jayatilaka, D. & Spackman, M. A. (2012). *Crystal Explorer*. The University of Western Australia.

supporting information

Acta Cryst. (2016). E**72**, 1121-1125 [https://doi.org/10.1107/S2056989016011026]

6-Methyl-2-oxo-*N*-(quinolin-6-yl)-2*H*-chromene-3-carboxamide: crystal structure and Hirshfeld surface analysis

Lígia R. Gomes, John Nicolson Low, André Fonseca, Maria João Matos and Fernanda Borges

Computing details

Data collection: GDA http://www.opengda.org/OpenGDA.html; cell refinement: XIA2 0.4.0.370-g47f3bc3, (Winter, 2010; data reduction: XIA2 0.4.0.370-g47f3bc3 (Winter, 2010; program(s) used to solve structure: SHELXT (Sheldrick, 2015a); program(s) used to refine structure: ShelXle (Hübschle *et al.*, 2011) *SHELXL2014*/7 (Sheldrick, 2015b); molecular graphics: *Mercury* (Macrae *et al.*, 2006); software used to prepare material for publication: *SHELXL2014*/17 (Sheldrick, 2015b) *PLATON* (Spek, 2009).

(I)

Crystal data

$C_{20}H_{14}N_2O_3$
M_r = 330.33
Monoclinic, $P2_1/n$
a = 7.799 (3) Å
b = 7.014 (3) Å
c = 27.640 (18) Å
β = 90.18 (6)°
V = 1512.0 (13) Å^3
Z = 4
$F(000)$ = 688
D_x = 1.451 Mg m^{-3}
Synchrotron′ radiation, λ = 0.68891 Å
Cell parameters from 3773 reflections
θ = 2.6–33.9°
μ = 0.09 mm^{-1}
T = 100 K
Needle, colourless
0.18 × 0.01 × 0.004 mm

Data collection

Three-circle diffractometer
Radiation source: synchrotron, DLS beamline I19, undulator
Si 111, double crystal monochromator
Detector resolution: 5.81 pixels mm^{-1}
profile data from ω–scans
Absorption correction: empirical (using intensity measurements) aimless ccp4 (Evans, 2006)
18408 measured reflections
4587 independent reflections
3717 reflections with $I > 2\sigma(I)$
R_{int} = 0.060
θ_{max} = 29.5°, θ_{min} = 2.9°
h = −11→11
k = −10→10
l = −39→39

Refinement

Refinement on F^2
Least-squares matrix: full
$R[F^2 > 2\sigma(F^2)]$ = 0.051
$wR(F^2)$ = 0.156
S = 1.13
4587 reflections
231 parameters
0 restraints
Hydrogen site location: mixed
H atoms treated by a mixture of independent and constrained refinement

$w = 1/[\sigma^2(F_o^2) + (0.0954P)^2]$
where $P = (F_o^2 + 2F_c^2)/3$
$(\Delta/\sigma)_{max} = 0.001$

$\Delta\rho_{max} = 0.54$ e Å^{-3}
$\Delta\rho_{min} = -0.25$ e Å^{-3}

Special details

Geometry. All esds (except the esd in the dihedral angle between two l.s. planes) are estimated using the full covariance matrix. The cell esds are taken into account individually in the estimation of esds in distances, angles and torsion angles; correlations between esds in cell parameters are only used when they are defined by crystal symmetry. An approximate (isotropic) treatment of cell esds is used for estimating esds involving l.s. planes.

Fractional atomic coordinates and isotropic or equivalent isotropic displacement parameters (Å²)

	x	*y*	*z*	U_{iso}*/U_{eq}
O1	0.61633 (10)	0.57511 (12)	0.33247 (3)	0.02193 (19)
O2	0.42390 (10)	0.67655 (12)	0.38475 (3)	0.0244 (2)
O31	0.79011 (10)	0.65810 (12)	0.49728 (3)	0.0240 (2)
N32	0.50968 (12)	0.71842 (13)	0.47835 (3)	0.0186 (2)
N311	0.21868 (12)	0.98576 (13)	0.65151 (3)	0.0204 (2)
C2	0.57274 (14)	0.62613 (16)	0.37867 (4)	0.0196 (2)
C3	0.70619 (13)	0.61438 (15)	0.41571 (4)	0.0177 (2)
C4	0.86585 (13)	0.55411 (15)	0.40316 (4)	0.0180 (2)
H4	0.9519	0.5451	0.4275	0.022*
C5	1.07250 (14)	0.44450 (15)	0.33910 (4)	0.0200 (2)
H5	1.1628	0.4362	0.3622	0.024*
C4A	0.90818 (14)	0.50369 (15)	0.35425 (4)	0.0182 (2)
C6	1.10480 (15)	0.39806 (16)	0.29103 (4)	0.0222 (2)
C7	0.97020 (15)	0.41362 (17)	0.25763 (4)	0.0238 (2)
H7	0.9904	0.3821	0.2247	0.029*
C8	0.80789 (15)	0.47398 (17)	0.27134 (4)	0.0230 (2)
H8	0.7184	0.4858	0.2482	0.028*
C8A	0.77937 (14)	0.51669 (16)	0.31972 (4)	0.0195 (2)
C31	0.67345 (13)	0.66578 (15)	0.46783 (4)	0.0185 (2)
C34A	0.18814 (13)	0.89163 (15)	0.56639 (4)	0.0176 (2)
C38A	0.28705 (13)	0.91692 (15)	0.60890 (4)	0.0178 (2)
C61	1.27981 (16)	0.3329 (2)	0.27477 (5)	0.0312 (3)
H61A	1.3103	0.2147	0.2916	0.047*
H61B	1.3647	0.4316	0.2824	0.047*
H61C	1.2781	0.3101	0.2398	0.047*
C312	0.05500 (14)	1.03063 (16)	0.65149 (4)	0.0219 (2)
H312	0.0075	1.0795	0.6806	0.026*
C313	−0.05445 (14)	1.01098 (16)	0.61122 (4)	0.0219 (2)
H313	−0.1717	1.0466	0.6133	0.026*
C314	0.01123 (13)	0.93934 (16)	0.56876 (4)	0.0199 (2)
H314	−0.0609	0.9220	0.5413	0.024*
C315	0.26757 (13)	0.82186 (15)	0.52375 (4)	0.0183 (2)
H315	0.2006	0.8037	0.4954	0.022*
C316	0.44016 (14)	0.78004 (15)	0.52286 (4)	0.0178 (2)
C317	0.53856 (14)	0.80040 (16)	0.56555 (4)	0.0197 (2)
H317	0.6569	0.7683	0.5655	0.024*

C318	0.46224 (14)	0.86712 (16)	0.60735 (4)	0.0198 (2)
H318	0.5297	0.8798	0.6358	0.024*
H32	0.440 (2)	0.709 (3)	0.4521 (6)	0.042 (5)*

Atomic displacement parameters (Å²)

	U^{11}	U^{22}	U^{33}	U^{12}	U^{13}	U^{23}
O1	0.0188 (4)	0.0271 (4)	0.0199 (4)	−0.0001 (3)	0.0003 (3)	−0.0025 (3)
O2	0.0186 (4)	0.0295 (5)	0.0250 (4)	0.0018 (3)	−0.0007 (3)	−0.0027 (3)
O31	0.0209 (4)	0.0295 (5)	0.0216 (4)	0.0024 (3)	−0.0005 (3)	−0.0043 (3)
N32	0.0184 (4)	0.0194 (5)	0.0180 (4)	0.0012 (3)	0.0018 (3)	−0.0009 (3)
N311	0.0226 (4)	0.0201 (5)	0.0186 (5)	−0.0011 (3)	0.0019 (3)	−0.0011 (3)
C2	0.0200 (5)	0.0186 (5)	0.0203 (5)	−0.0020 (4)	0.0014 (4)	−0.0007 (4)
C3	0.0185 (5)	0.0164 (5)	0.0183 (5)	−0.0012 (4)	0.0012 (4)	−0.0004 (4)
C4	0.0192 (5)	0.0155 (5)	0.0193 (5)	−0.0012 (4)	0.0008 (4)	0.0000 (4)
C5	0.0208 (5)	0.0178 (5)	0.0214 (5)	−0.0001 (4)	0.0019 (4)	−0.0001 (4)
C4A	0.0199 (5)	0.0154 (5)	0.0194 (5)	−0.0022 (4)	0.0021 (4)	−0.0006 (4)
C6	0.0242 (5)	0.0197 (5)	0.0227 (5)	−0.0012 (4)	0.0046 (4)	−0.0018 (4)
C7	0.0273 (5)	0.0240 (6)	0.0202 (5)	−0.0030 (4)	0.0042 (4)	−0.0024 (4)
C8	0.0248 (5)	0.0258 (6)	0.0185 (5)	−0.0030 (4)	−0.0011 (4)	−0.0013 (4)
C8A	0.0188 (5)	0.0193 (5)	0.0202 (5)	−0.0024 (4)	0.0021 (4)	−0.0007 (4)
C31	0.0194 (5)	0.0151 (5)	0.0212 (5)	−0.0009 (4)	0.0025 (4)	−0.0005 (4)
C34A	0.0178 (5)	0.0144 (5)	0.0205 (5)	−0.0002 (3)	0.0016 (4)	0.0011 (4)
C38A	0.0194 (5)	0.0158 (5)	0.0181 (5)	−0.0013 (4)	0.0016 (4)	0.0003 (4)
C61	0.0253 (6)	0.0408 (8)	0.0274 (6)	0.0069 (5)	0.0052 (5)	−0.0060 (5)
C312	0.0238 (5)	0.0204 (5)	0.0214 (5)	−0.0012 (4)	0.0057 (4)	−0.0012 (4)
C313	0.0188 (5)	0.0216 (5)	0.0251 (6)	0.0002 (4)	0.0032 (4)	0.0006 (4)
C314	0.0180 (5)	0.0202 (5)	0.0215 (5)	−0.0006 (4)	−0.0001 (4)	0.0015 (4)
C315	0.0195 (5)	0.0167 (5)	0.0188 (5)	0.0004 (4)	−0.0001 (4)	0.0003 (4)
C316	0.0201 (5)	0.0148 (5)	0.0185 (5)	−0.0001 (4)	0.0029 (4)	0.0006 (4)
C317	0.0183 (5)	0.0203 (5)	0.0206 (5)	0.0010 (4)	0.0016 (4)	0.0002 (4)
C318	0.0204 (5)	0.0207 (5)	0.0185 (5)	−0.0005 (4)	−0.0011 (4)	−0.0002 (4)

Geometric parameters (Å, º)

O1—C2	1.3701 (16)	C7—H7	0.9500
O1—C8A	1.3827 (14)	C8—C8A	1.3887 (18)
O2—C2	1.2255 (14)	C8—H8	0.9500
O31—C31	1.2201 (16)	C34A—C38A	1.4149 (18)
N32—C31	1.3618 (14)	C34A—C315	1.4200 (17)
N32—C316	1.4136 (16)	C34A—C314	1.4214 (15)
N32—H32	0.907 (18)	C38A—C318	1.4111 (16)
N311—C312	1.3147 (15)	C61—H61A	0.9800
N311—C38A	1.3814 (16)	C61—H61B	0.9800
C2—C3	1.4600 (18)	C61—H61C	0.9800
C3—C4	1.3609 (15)	C312—C313	1.4075 (19)
C3—C31	1.5075 (18)	C312—H312	0.9500
C4—C4A	1.4368 (17)	C313—C314	1.3769 (17)

C4—H4	0.9500	C313—H313	0.9500
C5—C6	1.3918 (18)	C314—H314	0.9500
C5—C4A	1.4119 (16)	C315—C316	1.3779 (15)
C5—H5	0.9500	C315—H315	0.9500
C4A—C8A	1.3866 (18)	C316—C317	1.4128 (18)
C6—C7	1.4000 (19)	C317—C318	1.3830 (17)
C6—C61	1.5092 (17)	C317—H317	0.9500
C7—C8	1.3886 (17)	C318—H318	0.9500

C2—O1—C8A	123.10 (10)	N32—C31—C3	115.51 (11)
C31—N32—C316	129.15 (11)	C38A—C34A—C315	119.63 (10)
C31—N32—H32	111.5 (11)	C38A—C34A—C314	117.32 (10)
C316—N32—H32	119.3 (11)	C315—C34A—C314	123.05 (11)
C312—N311—C38A	117.43 (11)	N311—C38A—C318	119.26 (11)
O2—C2—O1	116.17 (11)	N311—C38A—C34A	122.75 (10)
O2—C2—C3	126.42 (11)	C318—C38A—C34A	117.98 (10)
O1—C2—C3	117.42 (10)	C6—C61—H61A	109.5
C4—C3—C2	119.32 (11)	C6—C61—H61B	109.5
C4—C3—C31	118.40 (11)	H61A—C61—H61B	109.5
C2—C3—C31	122.28 (10)	C6—C61—H61C	109.5
C3—C4—C4A	121.96 (11)	H61A—C61—H61C	109.5
C3—C4—H4	119.0	H61B—C61—H61C	109.5
C4A—C4—H4	119.0	N311—C312—C313	124.28 (11)
C6—C5—C4A	121.27 (12)	N311—C312—H312	117.9
C6—C5—H5	119.4	C313—C312—H312	117.9
C4A—C5—H5	119.4	C314—C313—C312	118.92 (10)
C8A—C4A—C5	118.13 (11)	C314—C313—H313	120.5
C8A—C4A—C4	117.61 (11)	C312—C313—H313	120.5
C5—C4A—C4	124.25 (11)	C313—C314—C34A	119.27 (11)
C5—C6—C7	118.28 (11)	C313—C314—H314	120.4
C5—C6—C61	121.45 (12)	C34A—C314—H314	120.4
C7—C6—C61	120.28 (11)	C316—C315—C34A	121.13 (11)
C8—C7—C6	121.73 (11)	C316—C315—H315	119.4
C8—C7—H7	119.1	C34A—C315—H315	119.4
C6—C7—H7	119.1	C315—C316—C317	119.45 (11)
C7—C8—C8A	118.52 (12)	C315—C316—N32	117.26 (11)
C7—C8—H8	120.7	C317—C316—N32	123.29 (10)
C8A—C8—H8	120.7	C318—C317—C316	119.86 (10)
O1—C8A—C4A	120.59 (10)	C318—C317—H317	120.1
O1—C8A—C8	117.36 (11)	C316—C317—H317	120.1
C4A—C8A—C8	122.06 (11)	C317—C318—C38A	121.90 (11)
O31—C31—N32	124.57 (11)	C317—C318—H318	119.0
O31—C31—C3	119.91 (10)	C38A—C318—H318	119.0

C8A—O1—C2—O2	179.41 (9)	C4—C3—C31—O31	2.12 (16)
C8A—O1—C2—C3	−0.94 (15)	C2—C3—C31—O31	−178.23 (10)
O2—C2—C3—C4	179.54 (11)	C4—C3—C31—N32	−177.74 (9)
O1—C2—C3—C4	−0.06 (15)	C2—C3—C31—N32	1.91 (15)

O2—C2—C3—C31	−0.09 (18)	C312—N311—C38A—C318	179.98 (10)
O1—C2—C3—C31	−179.70 (9)	C312—N311—C38A—C34A	−0.77 (16)
C2—C3—C4—C4A	0.81 (16)	C315—C34A—C38A—N311	179.40 (10)
C31—C3—C4—C4A	−179.54 (9)	C314—C34A—C38A—N311	−0.32 (16)
C6—C5—C4A—C8A	−0.76 (16)	C315—C34A—C38A—C318	−1.34 (15)
C6—C5—C4A—C4	−179.86 (10)	C314—C34A—C38A—C318	178.94 (10)
C3—C4—C4A—C8A	−0.58 (16)	C38A—N311—C312—C313	0.74 (17)
C3—C4—C4A—C5	178.52 (10)	N311—C312—C313—C314	0.39 (18)
C4A—C5—C6—C7	0.76 (17)	C312—C313—C314—C34A	−1.51 (16)
C4A—C5—C6—C61	−179.40 (11)	C38A—C34A—C314—C313	1.45 (15)
C5—C6—C7—C8	0.15 (18)	C315—C34A—C314—C313	−178.25 (10)
C61—C6—C7—C8	−179.69 (11)	C38A—C34A—C315—C316	−0.68 (16)
C6—C7—C8—C8A	−1.03 (18)	C314—C34A—C315—C316	179.02 (10)
C2—O1—C8A—C4A	1.19 (16)	C34A—C315—C316—C317	2.29 (16)
C2—O1—C8A—C8	−178.25 (10)	C34A—C315—C316—N32	−177.58 (9)
C5—C4A—C8A—O1	−179.57 (9)	C31—N32—C316—C315	−178.87 (10)
C4—C4A—C8A—O1	−0.41 (15)	C31—N32—C316—C317	1.27 (18)
C5—C4A—C8A—C8	−0.15 (17)	C315—C316—C317—C318	−1.86 (16)
C4—C4A—C8A—C8	179.00 (10)	N32—C316—C317—C318	178.01 (10)
C7—C8—C8A—O1	−179.54 (10)	C316—C317—C318—C38A	−0.20 (17)
C7—C8—C8A—C4A	1.03 (18)	N311—C38A—C318—C317	−178.93 (10)
C316—N32—C31—O31	2.43 (19)	C34A—C38A—C318—C317	1.78 (16)
C316—N32—C31—C3	−177.72 (10)		

Hydrogen-bond geometry (Å, º)

D—H···*A*	*D*—H	H···*A*	*D*···*A*	*D*—H···*A*
C314—H314···O31^{i}	0.95	2.50	3.278 (2)	139
C8—H8···N311^{ii}	0.95	2.68	3.394 (3)	133
C317—H317···O31	0.95	2.29	2.903 (2)	122
N32—H32···O2	0.907 (18)	1.879 (18)	2.686 (2)	147.3 (15)

Symmetry codes: (i) *x*−1, *y*, *z*; (ii) *x*+1/2, −*y*+3/2, *z*−1/2.